HHS Public Access

Author manuscript

J Magn Reson. Author manuscript; available in PMC 2023 June 01.

Published in final edited form as:

J Magn Reson. 2022 June ; 339: 107230. doi:10.1016/j.jmr.2022.107230.

HIV-1 VIF and human APOBEC3G interaction directly observed through molecular specific labeling using a new dual promotor vector

Wazo Myint[a], **Celia A. Schiffer**[b], **Hiroshi Matsuo**[a,*]

[a] Basic Science Program, Frederick National Laboratory for Cancer Research, Frederick, Maryland 21702, USA

[b] Department of Biochemistry and Molecular Biotechnology, University of Massachusetts Chan Medical School, Worcester, MA, 01655, USA.

Abstract

Over the last few decades, protein NMR isotope labeling methods using *E. coli* based expression have revolutionized the information accessible from biomolecular NMR experiments. Selective labeling of a protein of interest in a multi-protein complex can significantly reduce the number of cross-peaks and allow for study of large protein complexes. However, limitations still remain since some proteins are not stable independently and cannot be separately labeled in either NMR active isotope enriched or unenriched media and reconstituted into a multimeric complex. To overcome this limitation, the LEGO-NMR method was previously developed using protein expression plasmids containing T7 or araBAD promoters to separately express proteins in the same *E. coli* after changing between labeled and unlabeled media.

Building on this, we developed a method to label the Human Immunodeficiency Virus type 1 viral infectivity factor (HIV-1 Vif), a monomerically unstable protein, in complex with CBFβ, it's host binding partner. We designed a dual promoter plasmid containing both T7 and araBAD promoters to independently control the expression of HIV-1 Vif in NMR active isotope enriched media and CBFβ in unenriched media. Using this method, we assigned the backbone resonance and directly observed the binding of HIV-1 Vif with APOBEC3G, a host restriction factor to HIV-1.

Graphical Abstract

* To whom correspondence should be addressed. Tel: +1 (301) 228-4375, hiroshi.matsuo@nih.gov.

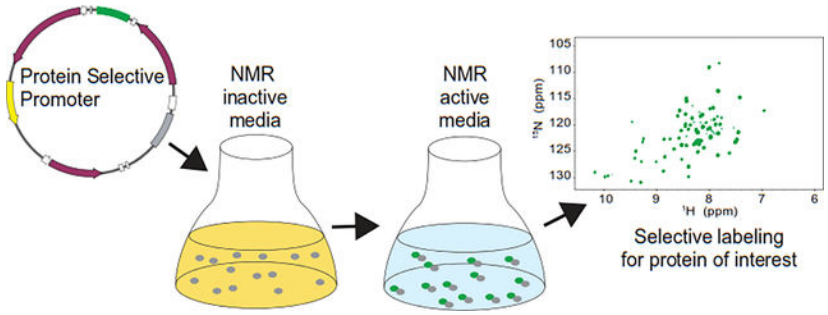

Introduction

Stable-isotope labeling can be a limitation in studying biomolecules using NMR spectroscopy, yet sometimes it provides a tool to obtain atomic-level details of complicated biological systems. An example of such good use of stable-isotope labeling is molecular selective labeling of the protein of interest in a large multiprotein complex, which allows the researcher to observe NMR signals only from the labeled molecule and reduces complexity of NMR spectra. The molecular selective labeling becomes difficult to achieve if the multi-protein complex cannot be reconstituted by using separately purified proteins and all proteins need to be expressed in a single cell to form a proper complex. LEGO-NMR method had been developed by Dr. Sprangers's group in which the plasmid containing an araBAD promotor (arabinose inducible) and the plasmid containing a T7 promotor were co-transformed in *E. coli*, and proteins were separately induced in stable-isotope enriched medium or unlabeled medium, resulting in selective-isotope labeling of a protein of interest in a large heteromeric complex[1]. Following the LEGO-NMR principle and we generated a new plasmid that contained both araBAD and T7 promotors using the pETDuet-1vector (Novagen) as a template. This new vector, called araBAD-pETDuet-1 hereafter, was used to express the Vif protein of human immunodeficiency virus type 1 (HIV-1) and human core-binding factor subunit β (CBFβ) protein in *E. coli* to produce stable-isotope labeled Vif forming a complex with unlabeled CBFβ. Vif is one of six accessary proteins of HIV-1, and it helps infection of the virus by trigering degradation of the human antiretroviral APOBEC3 proteins including APOBEC3D, 3F, 3G and 3H [2–4]. Without Vif, these antiretrovieral APOBEC3 proteins are encapsidated into budding virions, then within the viral capsid they mutate cytidines to deoxy-uridines in the newly synthesiszed minus-strand of viral DNA [5]. In order to trigger the degradation, Vif forms a ubiquitin E3-ligase complex and targets these anti-HIV-1 APOBEC3 proteins for ubiquitylation, then degradation through proteasome. [6] [7] [8] As Vif is insoluble in isolation *in vitro* and unstable without binding the host binding partner CBFβ in human cells, coexpression of Vif with CBFβ in *E. coli* is necessary to purify the Vif-CBFβ complex [9] [10] [11]. One caveat was that the isolated Vif-CBFβ complex was not soluble enough for NMR spectroscopy. Therefore, we generated a deletion variant of Vif (ΔVif) that was more soluble than wildtype to yield a soluble ΔVif-CBFβ complex. After establishing the co-expression system of ΔVif and CBFβ using the araBAD-pETDuet-1 vector, NMR samples of the ΔVif-CBFβ complex were made containing stable-isotope including ^{13}C, ^{15}N and ^{2}H labeled ΔVif and unlabeled CBFβ and assigned mainchain atoms using conventional triple-resonance NMR spectra [12]

[13] [14] [15] [16] [17] [18] [19] [20] [21] [22] [23] [24]. Vif must bind the APOBEC3 proteins as a part of the ubiquitin E3-ligase complex for ubiquitylation. We used human APOBEC3G protein (A3G) that provided most potent restrition of the HIV-1 infection to map Vif residues which were involved in A3G interaction by using ^{1}H-^{15}N TROSY-HSQC spectra [24] [23] [21] [22] [20] [25]. The mapped residues agreed with the residues that had been identified by indirect observations including mutations, coimmunoprecipitation, and *in vivo* degradation assays [26] [27] [28] [29] [30] [31] [32] [33] [34]. The newly generated araBAD-pETDuet-1 vector enabled purification of the ΔVif-CBFβ complex and selective observation of ΔVif NMR signals, which resulted in the direct observation of a Vif-APOBEC3 interaction.

Results

Design of soluble Vif and CBFβ complex

The crystal structure of Vif was used in the design of a soluble variant (PDB ID: 4N9F[35]). Figure 1a shows the region (residues 112 to 163 highlighted in cyan) including the zinc finger that binds Cullin5 and the BC-box that binds the Elongin B and Elongin C complex were replaced with a 3 residue GSS linker and the resulting construct was named ΔVif. The Cul5 interacting N-terminal tail (residues 1 to 4 also in cyan) of the CBFβ binding partner was also truncated to increase protein solubility and named ΔCBFβ.

Design of araBAD-pETDuet-1 vector for specific labeling of ΔVif

A new vector that contained an arabinose inducible promotor (araBAD) and T7 promotor was constructed by using pETDuet-1 vector (Novagen) and pBAD vector (ThermoFisher Scientific) as templates. The araBAD promotor and the araC gene from pBAD were subcloned to replace the second T7 promotor region of pETDuet-1 (Figure 1b). In the absence of L-arabinose, the araC transcription product prevents transcription initiation from the araBAD by forming a DNA loop that prevents RNA polymerase binding. [36] This loop is released on L-arabinose binding to araC. The resulting vector is called araBAD-pETDuet-1, hereafter. The ΔVif and ΔCBFβ genes were subcloned under the T7 and araBAD promotors, respectively. The resulting 6295 base pair plasmid enabled us to express ΔCBFβ first by addition of L-arabinose (Figure 1c). Expression of ΔCBFβ can be stopped by removal of L-arabinose from the medium and addition of D-glucose. D-glucose reduces the levels of 3',5'-cyclic AMP (cAMP) and therefore inhibits expression of the catabolite-repressed araBAD promotor. [37] The tight control of ΔCBFβ expression resulted in no free ΔCBFβ cross peaks in the ^{1}H-^{15}N TROSY-HSQC spectra. Cells were spun down and resuspended in growth media containing stable-isotopes to express ΔVif. This expression order is important since ΔVif would be aggregated in cells if it cannot form a complex with ΔCBFβ [9] [10].

Although *araBAD-pETDuet-1* vector contains one copy of *ΔVif and ΔCBFβ gene,* the expression of these proteins may not be 1:1 because the amounts of expressed protein in cells are affected by promotor strength, translation efficiency, and protein stability. Therefore, optimization of these conditions for each protein is very important. Our dual-

promotor single plasmid approach has an advantage compared to using two single plasmids as follows.

Using a single plasmid containing both ΔVif and ΔCBFβ only required a single antibiotic selection and a single transformation protocol. Compared with multi-antibiotics required to transform two plasmids, the single antibiotic selection keeps *E. coli* cells healthier and viable during the growth in minimal media especially with deuterium. Using two plasmids for expression of two proteins usually requires two separate transformations including the first transformation to make competent cells with one plasmid and another transformation with the second plasmid, as a consequence the ratio of the two plasmids in the *E. coli* cell cannot be precisely controlled. This makes optimizing conditions for protein expression difficult since using the same expression conditions in different experiments can potentially yield different ratios of the expressed proteins. This is exacerbated by the differences in promotors since T7 promotor has much stronger expression in comparison to araBAD. [38]

Using only araBAD-pETDuet-1 vector, this uncertainty could be eliminated, which enabled us to optimize other parameters for protein expression including the concentration of inducers, induction times, temperature during induction and concentration of stable-isotopes. The optimization of these parameters was important for expressing the ΔVif protein to avoid aggregation of ΔVif in cells by ensuring that optimized amount of ΔCBFβ was expressed before the ΔVif expression.

Isotope enrichment of ΔVif in the ΔVif-ΔCBFβ complex

BL21(DE3) chemically competent *E. coli* were transformed with araBAD-pETDuet-1 plasmid containing ΔVif and ΔCBFβ and grown in either Terrific Broth (NMR inactive) or stable isotope enriched media (NMR active) until OD 0.1 at 37°C. Overexpression of ΔCBFβ was induced by addition of L-arabinose to 0.2% w/v concentration and incubated for 3 hours. For NMR inactive or uniformly labeled protein, temperature was reduced to 16°C and 0.2mM IPTG was added to induce overexpression of ΔVif. The concentrations of inducing reagents, durations, and temperatures of induction were optimized for ΔCBFβ expression first and then for ΔVif expression. Cells were harvested by centrifugation at 5000×g for 20 minutes and pellets were stored in −80°C until needed.

For NMR active ΔVif, D-glucose was added to 0.5% w/v concentration to stop ΔCBFβ overexpression and incubated for 20 minutes before centrifugation at 1500×g for 20 minutes. Cell pellets were resuspended in either ^{15}N or $^{15}N/^{13}C$ (in 85% D_2O) enriched Bioexpress Cell Growth media (Cambridge Isotope Laboratories, Inc. Tewksbury, MA) at 16°C and overexpression of ΔVif was induced for 12 hours by addition of 0.2 mM IPTG (Figure 1c). This NMR active ΔVif and NMR inactive ΔCBFβ will be referred to as $\Delta Vif^{NMR\ active}$-$\Delta CBF\beta^{NMR\ inactive}$. For specific amino acid labeling of ΔVif, the growth media was replaced by minimal M9 media enriched with 150 mg/L of alanine, arginine, asparagine, aspartic acid, cysteine, glutamine, glutamic acid, glycine, histidine, isoleucine, leucine, lysine, methionine, phenylalanine, proline, serine, threonine, tyrosine, valine, and 200 mg/L of tryptophan. In place of naturally abundant amino acids, ^{15}N enriched valine, tyrosine, threonine, serine, lysine, leucine, histidine, or alanine was substituted in the growth media to identify the amino acid type of ^{15}N-^{1}H resonances.

Resonance assignment of ΔVif

Overlaying the ^{1}H-^{15}N TROSY-HSQC spectra of uniformly ^{15}N enriched ΔVif-ΔCBFβ complex and the complex with only ΔVif labeled show that the number of cross-peaks are significantly reduced (Figure 2a), since cross-peaks from both the free ΔCBFβ and the ΔVif bound ΔCBFβ were eliminated. The control of ΔCBFβ expression by the araBAD promoter resulted in very little leakage of labeled ΔCBFβ and cross peaks originating from both ΔVif bound and free ΔCBFβ were not observed. We were also able to isotopically enrich ΔVif by specific amino acid type (Figure 2b). The overlay of the uniformly enriched ΔVif spectrum (black single contour outline) with amino acid type specific spectra (colored spectra with enriched amino acid types indicated in the figure) demonstrates that the expression method can be successfully applied to various type of labeling media. Protein backbone resonance assignment using traditional three dimensional spectra and specific amino acid type labeled spectra (Figure 2b) yielded in 76% of observed cross peaks being assigned (Figure 3).

Chemical shift perturbation on addition of A3G NTD-CTD2EA Y125A

For identification of the HIV-1 Vif amino acid residues interacting with A3G, we used a soluble variant of the A3G C-terminal domain (CTD2EA [39]) and the Vif binding N-terminal domain with a Y125A mutation (referred to as A3G NTD-CTD2EA Y125A). The Y125A mutation was designed to reduce multimerization/aggregation of A3G since the aggregation prevents the interaction with Vif. The ^{1}H-^{15}N TROSY-HSQC spectra of 100μM $\Delta Vif^{NMR\ active}$-$\Delta CBF\beta^{NMR\ inactive}$ complex in the absence and presence of 10 μM NMR inactive A3G NTD-CTD2EA Y125A (a ratio of 1:10) were overlaid, Figure 4a, to determine which ΔVif amino acid residues show interaction with A3G. Both surface (green labels) and interior (purple labels) residues were perturbed on interaction with A3G. Surface residues H43 and Y44 are shown in green stick model, while interior residues are shown in purple stick model on the structure of ΔVif-ΔCBFβ, Figure 4b. Interior residues V25, H56, I66, T67, T68 and Y69 that show chemical shift perturbation are located primarily in the beta sheet forming the core of the protein structure. *Nota bene*, we could not use higher concentration of A3G NTD-CTD2EA Y125A than 10 μM because NMR spectra started to show signs of protein aggregation.

Discussion and conclusion

The interaction between HIV-1 Vif and human A3G has been studied using co-immunoprecipitation and degradation assays, and Vif residues 21–26, 40–44 and 64–72 were identified to be involved in complex formation [26] [27] [40] [29] [30] [32] [33]. Yet the direct observation of the Vif-A3G interaction using biophysical or structural methods has been hampered due to the insolubility and structural complexity of the A3G and Vif samples. To overcome these challenges, we first engineered the smallest and most soluble Vif by forming a complex with CBFβ (the ΔVif-ΔCBFβ complex). The ΔVif still retains the aforementioned three regions which had been suggested to be involved in the A3G interaction.

Using the optimized double-promotor expression strategy, we were able to perform resonance assignment on the $\Delta Vif^{NMR\ active}$-$\Delta CBF\beta^{NMR\ inactive}$ complex and identify the

Vif surface residues which were most likely involved in direct interaction with A3G. Vif residues 40–44 had arguably the strongest experimental evidence to be involved in specific interaction with A3G as alanine mutation of these residues severely reduced co-immunoprecipitation with A3G [27]. Our NMR results indicate that both H43 and Y44 directly interact A3G. Although Vif residues 21–26, specifically K26 and a lesser extent K22, have been suggested to be important for the Vif-induced degradation of A3G [29] [30], neither K22 nor K26 showed significant chemical shift perturbation in our NMR binding experiment. These apparently conflicting results could be due to the low concentration of A3G NTD-CTD2EA Y125A (10μM) used in our NMR binding experiment, which allowed us to see the initiation of the Vif-A3G interaction. Since negatively charged surface of A3G-NTD including loop-7 has been suggested to be important for Vif binding [41] [42], it is plausible that positively charged surface residues such as K22 and K26 interact with A3G at higher concentration to form tighter complex.

Fascinatingly, interior residues I66, T67, T68 and Y69 were perturbed upon addition of A3G NTD-CTD2EA Y125A at this concentration (Figure 4c). These residues form a beta strand and they are in the center of the 64–72 region that had been suggested to be important for the Vif-induced degradation of A3G [43]. Given these results the core structure of Vif undergoes conformational changes upon the first contact with H43 and Y44 of A3G. This dynamical behavior of ΔVif is a new observation that only could be captured by NMR and may provide insights into this important recognition event.

Building on the pioneering work done by Dr. Sprangers's group, we generated a new dual-promotor vector that enabled us to specifically observe only the Vif NMR signals in the ΔVif-ΔCBFβ complex. Our *araBAD-pETDuet-1* vector showed excellent suppression of NMR-inactive protein, and it could be generally useful for generating two protein complexes where one protein must stabilize the second protein.

In comparison, cell free protein expression and labeling methods would require expression of the labeled protein in the presence of its purified stable binding partner. This necessitates separate expression using unlabeled media and purification since mixing with unpurified cell lysate would lead to introduction of unlabeled reagents into the cell free system and greatly diminish labeling efficiency. Our method skips this step by performing the overexpression and media changes in cell. This would save time and effort. In addition, NMR active stable isotope enriched protein production using *E. coli* systems are well established in research groups using biomolecular NMR spectroscopy, therefore many laboratories can use our dual-promotor vector for generation of their protein complexes.

As we have shown, this expression strategy can be applied further towards specific amino acid labeling, or also for methyl labeling to allow for study of larger complexes. This work adds to the compendium of available strategies for selective and specific isotope labeling of proteins for biomolecular NMR.

Methods

Purification of proteins.

Amino acid sequences of ΔVif and A3G NTD-Y125A-CTD2EA are provided in Supplementary Figure 1. Purification of the $\Delta Vif^{NMR\ active}$-$\Delta CBF\beta^{NMR\ inactive}$ complex. Cell pellets were resuspended in lysis buffer (25 mM Tris pH 7.3, 250 mM NaCl, 0.01% w/v TWEEN20, 1 mM DTT, and 40 mM Immidazole.) and lysis was performed using Avestin C3 homogenizer. Cell debris was separated by centrifugation at 48,000×g for 30 minutes. Lysate was bound to equilibrated Ni-NTA resin and batch purification was performed by washing with high salt buffer (25 mM Tris pH 7.3, 3000 mM NaCl, 0.01% w/v TWEEN20, and 1 mM DTT), low salt buffer (25 mM Tris pH 7.3, 1500 mM NaCl, 0.01% w/v TWEEN20, and 1 mM DTT), and three times with 25 mM Tris pH 7.3, 250 mM NaCl, 0.01% w/v TWEEN20, and 1 mM DTT. Protein was eluted in elution buffer (25 mM Tris pH 7.3, 250 mM NaCl, 0.01% w/v TWEEN20, 1 mM DTT, and 400 mM Immidazole.) and further purified through Superdex75 HiLoad equilibrated with NMR buffer (25 mM Tris pH 7.3, 100 mM NaCl, 0.002% w/v TWEEN20, 1 mM DTT, and 50 mM Choline-O-sulfate). The expression and purification of the A3G NTD-Y125A-CTD2EA was performed as previously described. Purified A3G NTD-CTD2EA Y125A in 25 mM Tris pH 7.3, 100 mM NaCl, 0.002% w/v TWEEN20, 1 mM DTT, and 500 mM Choline-O-sulfate was added to the NMR sample to a concentration of 15μM and final ΔVif-ΔCBFβ concentration was at 100μM.

NMR Spectroscopy

NMR experiments were performed on Bruker NMR spectrometers operating at ^{1}H Larmor frequencies of 800MHz and 850MHz. ΔVif-ΔCBFβ spectra for resonance assignment were measured at 40°C with protein concentrations of 150 to 200μM in 5mm Shigemi tubes.

TROSY versions of triple resonance experiments were performed for backbone resonance assignment: HNCA, HN(CO)CA, HNCACB, HNCO, HN(CA)CO, and ^{15}N-^{1}H HSQC [12] [13] [14] [15] [16].

Supplementary Material

Refer to Web version on PubMed Central for supplementary material.

Funding

This work was supported in part by a grant from the U.S. National Institutes of Health R01GM118474/R01AI150478 for CAS and HM. For WM and HM, this project has been funded in part with federal funds from the National Cancer Institute, National Institutes of Health, under contract 75N91019D00024. WM was supported in part by the NIH Office of Intramural Training and Education's Intramural AIDS Research Fellowship. The content of this publication does not necessarily reflect the views or policies of the Department of Health and Human Services, nor does mention of trade names, commercial products, or organizations imply endorsement by the U.S. Government.

Declaration of interests

The authors declare the following financial interests/personal relationships which may be considered as potential competing interests:

Hiroshi Matsuo reports financial support was provided by National Institutes of Health. Celia A. Schiffer reports financial support was provided by National Institutes of Health. Wazo Myint reports financial support was provided by NIH office of intramural training and education.

References

[1]. Mund M, Overbeck JH, Ullmann J, Sprangers R. LEGO-NMR Spectroscopy: A Method to Visualize Individual Subunits in Large Heteromeric Complexes. Angewandte Chemie International Edition. 2013;52:11401–5. doi:10.1002/anie.201304914 [PubMed: 23946163]

[2]. Sheehy AM, Gaddis NC, Choi JD, Malim MH. Isolation of a human gene that inhibits HIV-1 infection and is suppressed by the viral Vif protein. Nature. 2002;418:646–50. doi:10.1038/nature00939 [PubMed: 12167863]

[3]. Conticello SG, Harris RS, Neuberger MS. The Vif Protein of HIV Triggers Degradation of the Human Antiretroviral DNA Deaminase APOBEC3G. Current Biology. 2003;13:2009–13. doi:10.1016/j.cub.2003.10.034

[4]. Mariani R, Chen D, Schröfelbauer B, Navarro F, König R, Bollman B, et al. Species-Specific Exclusion of APOBEC3G from HIV-1 Virions by Vif. Cell. 2003;114:21–31. doi:10.1016/S0092-8674(03)00515-4 [PubMed: 12859895]

[5]. Lecossier D, Bouchonnet F, Clavel F, Hance Allan J. Hypermutation of HIV-1 DNA in the Absence of the Vif Protein. Science. 2003;300:1112-. doi:10.1126/science.1083338 [PubMed: 12750511]

[6]. Marin M, Rose KM, Kozak SL, Kabat D. HIV-1 Vif protein binds the editing enzyme APOBEC3G and induces its degradation. Nature Medicine. 2003;9:1398–403. doi:10.1038/nm946

[7]. Sheehy AM, Gaddis NC, Malim MH. The antiretroviral enzyme APOBEC3G is degraded by the proteasome in response to HIV-1 Vif. Nature Medicine. 2003;9:1404–7. doi:10.1038/nm945

[8]. Yu X, Yu Y, Liu B, Luo K, Kong W, Mao P, et al. Induction of APOBEC3G Ubiquitination and Degradation by an HIV-1 Vif-Cul5-SCF Complex. Science. 2003;302:1056–60. doi:10.1126/science.1089591 [PubMed: 14564014]

[9]. Jäger S, Kim DY, Hultquist JF, Shindo K, LaRue RS, Kwon E, et al. Vif hijacks CBF-β to degrade APOBEC3G and promote HIV-1 infection. Nature. 2012;481:371–5. doi:10.1038/nature10693

[10]. Zhang W, Du J, Evans SL, Yu Y, Yu X-F. T-cell differentiation factor CBF-β regulates HIV-1 Vif-mediated evasion of host restriction. Nature. 2012;481:376–9. doi:10.1038/nature10718

[11]. Kim DY, Kwon E, Hartley PD, Crosby DC, Mann S, Krogan NJ, et al. CBFbeta stabilizes HIV Vif to counteract APOBEC3 at the expense of RUNX1 target gene expression. Mol Cell. 2013;49:632–44. doi:10.1016/j.molcel.2012.12.012 [PubMed: 23333304]

[12]. Ikura M, Kay LE, Bax A. A novel approach for sequential assignment of proton, carbon-13, and nitrogen-15 spectra of larger proteins: heteronuclear triple-resonance three-dimensional NMR spectroscopy. Application to calmodulin. Biochemistry. 1990;29:4659–67. doi:10.1021/bi00471a022 [PubMed: 2372549]

[13]. Kay LE, Ikura M, Tschudin R, Bax A. Three-dimensional triple-resonance NMR spectroscopy of isotopically enriched proteins. Journal of Magnetic Resonance (1969). 1990;89:496–514. doi:10.1016/0022-2364(90)90333-5

[14]. Yamazaki T, Lee W, Arrowsmith CH, Muhandiram DR, Kay LE. A Suite of Triple Resonance NMR Experiments for the Backbone Assignment of 15N, 13C, 2H Labeled Proteins with High Sensitivity. Journal of the American Chemical Society. 1994;116:11655–66. doi:10.1021/ja00105a005

[15]. Matsuo H, Li H, Wagner G. A Sensitive HN(CA)CO Experiment for Deuterated Proteins. Journal of Magnetic Resonance, Series B. 1996;110:112–5. doi:10.1006/jmrb.1996.0018 [PubMed: 8556234]

[16]. Salzmann M, Pervushin K, Wider G, Senn H, Wüthrich K. TROSY in triple-resonance experiments: New perspectives for sequential NMR assignment of large proteins. Proceedings of the National Academy of Sciences. 1998;95:13585. doi:10.1073/pnas.95.23.13585

[17]. Eletsky A, Kienhöfer A, Pervushin K. TROSY NMR with partially deuterated proteins. Journal of Biomolecular NMR. 2001;20:177–80. doi:10.1023/A:1011265430149 [PubMed: 11495249]

[18]. Salzmann M, Wider G, Pervushin K, Senn H, Wüthrich K. TROSY-type Triple-Resonance Experiments for Sequential NMR Assignments of Large Proteins. Journal of the American Chemical Society. 1999;121:844–8. doi:10.1021/ja9834226

[19]. Schulte-Herbrüggen T, Sørensen OW. Clean TROSY: Compensation for Relaxation-Induced Artifacts. Journal of Magnetic Resonance. 2000;144:123–8. doi:10.1006/jmre.2000.2020 [PubMed: 10783281]

[20]. Zhu G, Kong XM, Sze KH. Gradient and sensitivity enhancement of 2D TROSY with water flip-back, 3D NOESY-TROSY and TOCSY-TROSY experiments. Journal of Biomolecular NMR. 1999;13:77–81. doi:10.1023/A:1008398227519 [PubMed: 21080266]

[21]. Rance M, Loria JP, Palmer AG. Sensitivity Improvement of Transverse Relaxation-Optimized Spectroscopy. Journal of Magnetic Resonance. 1999;136:92–101. doi:10.1006/jmre.1998.1626 [PubMed: 9887294]

[22]. Weigelt J. Single Scan, Sensitivity- and Gradient-Enhanced TROSY for Multidimensional NMR Experiments. Journal of the American Chemical Society. 1998;120:10778–9. doi:10.1021/ja982649y

[23]. Pervushin KV, Wider G, Wüthrich K. Single Transition-to-single Transition Polarization Transfer (ST2-PT) in [15N,1H]-TROSY. Journal of Biomolecular NMR. 1998;12:345–8. doi:10.1023/A:1008268930690 [PubMed: 21136330]

[24]. Czisch M, Boelens R. Sensitivity Enhancement in the TROSY Experiment. Journal of Magnetic Resonance. 1998;134:158–60. doi:10.1006/jmre.1998.1483 [PubMed: 9740742]

[25]. Pervushin K, Riek R, Wider G, Wüthrich K. Attenuated T2 relaxation by mutual cancellation of dipole–dipole coupling and chemical shift anisotropy indicates an avenue to NMR structures of very large biological macromolecules in solution. Proceedings of the National Academy of Sciences. 1997;94:12366. doi:10.1073/pnas.94.23.12366

[26]. Mehle A, Wilson H, Zhang C, Brazier Andrew J, McPike M, Pery E, et al. Identification of an APOBEC3G Binding Site in Human Immunodeficiency Virus Type 1 Vif and Inhibitors of Vif-APOBEC3G Binding. Journal of Virology. 2007;81:13235–41. doi:10.1128/JVI.00204-07 [PubMed: 17898068]

[27]. Russell RA, Pathak VK. Identification of two distinct human immunodeficiency virus type 1 Vif determinants critical for interactions with human APOBEC3G and APOBEC3F. J Virol. 2007;81:8201–10. doi:10.1128/JVI.00395-07 [PubMed: 17522216]

[28]. Yamashita T, Kamada K, Hatcho K, Adachi A, Nomaguchi M. Identification of amino acid residues in HIV-1 Vif critical for binding and exclusion of APOBEC3G/F. Microbes and Infection. 2008;10:1142–9. doi:10.1016/j.micinf.2008.06.003 [PubMed: 18603011]

[29]. Chen G, He Z, Wang T, Xu R, Yu X-F. A Patch of Positively Charged Amino Acids Surrounding the Human Immunodeficiency Virus Type 1 Vif SLVx4Yx9Y Motif Influences Its Interaction with APOBEC3G. Journal of Virology. 2009;83:8674–82. doi:10.1128/JVI.00653-09 [PubMed: 19535450]

[30]. Dang Y, Wang X, Zhou T, York Ian A, Zheng Y-H. Identification of a Novel WxSLVK Motif in the N Terminus of Human Immunodeficiency Virus and Simian Immunodeficiency Virus Vif That Is Critical for APOBEC3G and APOBEC3F Neutralization. Journal of Virology. 2009;83:8544–52. doi:10.1128/JVI.00651-09 [PubMed: 19535447]

[31]. Tian C, Yu X, Zhang W, Wang T, Xu R, Yu X-F. Differential Requirement for Conserved Tryptophans in Human Immunodeficiency Virus Type 1 Vif for the Selective Suppression of APOBEC3G and APOBEC3F. Journal of Virology. 2006;80:3112–5. doi:10.1128/JVI.80.6.3112-3115.2006 [PubMed: 16501124]

[32]. He Z, Zhang W, Chen G, Xu R, Yu X-F. Characterization of Conserved Motifs in HIV-1 Vif Required for APOBEC3G and APOBEC3F Interaction. Journal of Molecular Biology. 2008;381:1000–11. doi:10.1016/j.jmb.2008.06.061 [PubMed: 18619467]

[33]. Pery E, Rajendran Kottampatty S, Brazier Andrew J, Gabuzda D. Regulation of APOBEC3 Proteins by a Novel YXXL Motif in Human Immunodeficiency Virus Type 1 Vif and Simian Immunodeficiency Virus SIVagm Vif. Journal of Virology. 2009;83:2374–81. doi:10.1128/JVI.01898-08 [PubMed: 19109396]

[34]. Kitamura S, Ode H, Nakashima M, Imahashi M, Naganawa Y, Kurosawa T, et al. The APOBEC3C crystal structure and the interface for HIV-1 Vif binding. Nature Structural & Molecular Biology. 2012;19:1005–10. doi:10.1038/nsmb.2378

[35]. Guo Y, Dong L, Qiu X, Wang Y, Zhang B, Liu H, et al. Structural basis for hijacking CBF-β and CUL5 E3 ligase complex by HIV-1 Vif. Nature. 2014;505:229–33. doi:10.1038/nature12884 [PubMed: 24402281]

[36]. Lobell Robert B, Schleif Robert F. DNA Looping and Unlooping by AraC Protein. Science. 1990;250:528–32. doi:10.1126/science.2237403 [PubMed: 2237403]

[37]. Guzman LM, Belin D, Carson MJ, Beckwith J. Tight regulation, modulation, and high-level expression by vectors containing the arabinose PBAD promoter. Journal of Bacteriology. 1995;177:4121–30. doi:10.1128/jb.177.14.4121-4130.1995 [PubMed: 7608087]

[38]. Samuelson J Bacterial Systems. Production of Membrane Proteins. 2011:11–35. doi:doi.org/10.1002/9783527634521.ch1

[39]. Maiti A, Myint W, Kanai T, Delviks-Frankenberry K, Sierra Rodriguez C, Pathak VK, et al. Crystal structure of the catalytic domain of HIV-1 restriction factor APOBEC3G in complex with ssDNA. Nat Commun. 2018;9:2460. doi:10.1038/s41467-018-04872-8 [PubMed: 29941968]

[40]. Yamashita T, Nomaguchi M, Miyake A, Uchiyama T, Adachi A. Status of APOBEC3G/F in cells and progeny virions modulated by Vif determines HIV-1 infectivity. Microbes Infect. 2010;12:166–71. doi:10.1016/j.micinf.2009.11.007 [PubMed: 19944180]

[41]. Kouno T, Luengas EM, Shigematsu M, Shandilya SM, Zhang J, Chen L, et al. Structure of the Vif-binding domain of the antiviral enzyme APOBEC3G. Nat Struct Mol Biol. 2015;22:485–91. doi:10.1038/nsmb.3033 [PubMed: 25984970]

[42]. Lavens D, Peelman F, Van der Heyden J, Uyttendaele I, Catteeuw D, Verhee A, et al. Definition of the interacting interfaces of Apobec3G and HIV-1 Vif using MAPPIT mutagenesis analysis. Nucleic Acids Res. 2010;38:1902–12. doi:10.1093/nar/gkp1154 [PubMed: 20015971]

[43]. He Z, Zhang W, Chen G, Xu R, Yu XF. Characterization of conserved motifs in HIV-1 Vif required for APOBEC3G and APOBEC3F interaction. J Mol Biol. 2008;381:1000–11. doi:10.1016/j.jmb.2008.06.061 [PubMed: 18619467]

[44]. Adachi A, Gendelman HE, Koenig S, Folks T, Willey R, Rabson A, et al. Production of acquired immunodeficiency syndrome-associated retrovirus in human and nonhuman cells transfected with an infectious molecular clone. Journal of virology. 1986;59:284–91. doi:10.1128/JVI.59.2.284-291.1986 [PubMed: 3016298]

Highlights

- Selective labeling of a protein of interest allows for NMR based study of large molecular complexes.
- Monomerically unstable HIV-1 VIF can be selectively labeled by expression of unlabeled binding partner before changing to NMR labeling media and inducing expression of VIF.
- Application of the method to HIV-1 VIF allowed for mapping of the HIV-1 restriction factor APOBEC3G binding site.

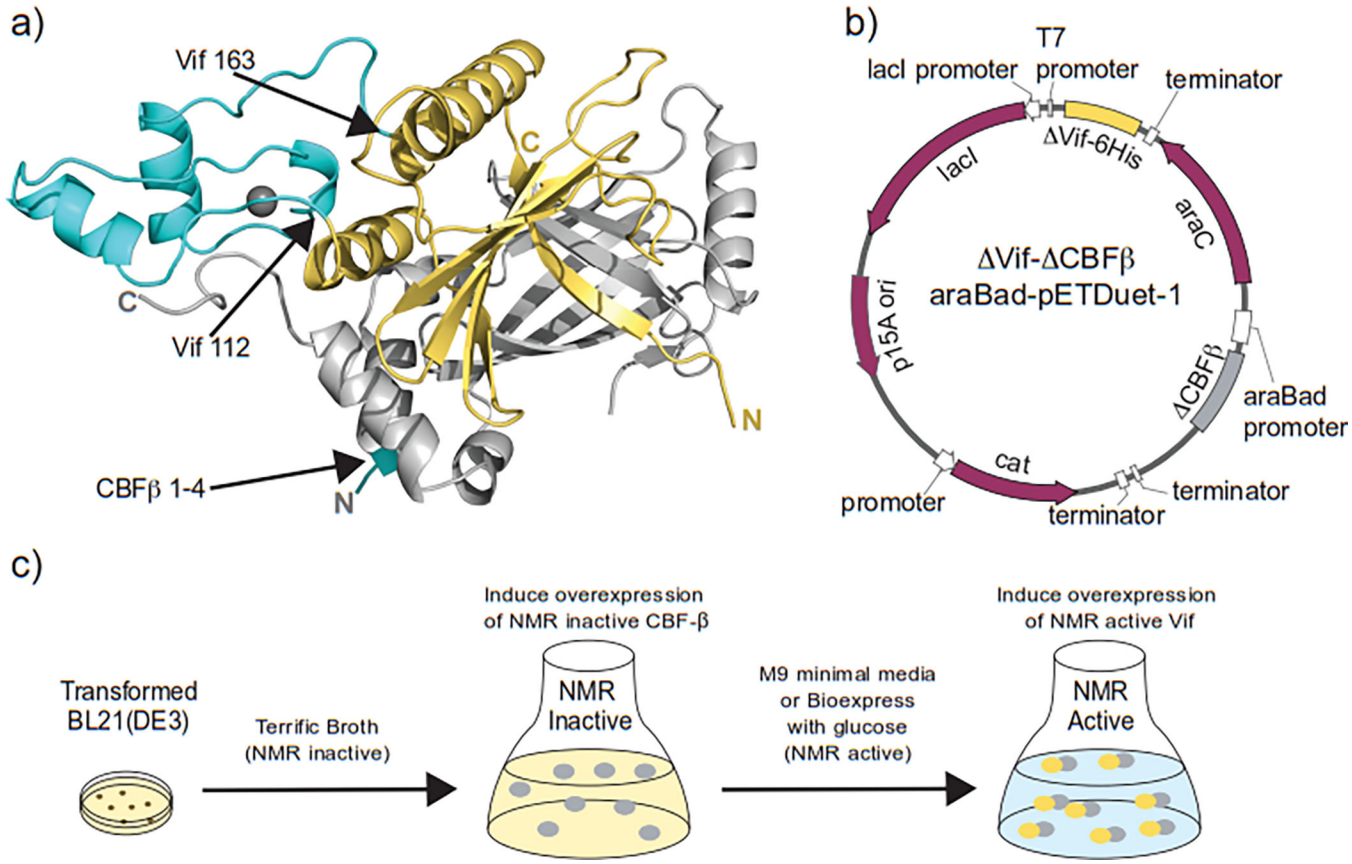

Figure 1.

a) Soluble HIV-1 ΔVif (yellow) in complex with ΔCBFβ (grey) was designed based on the crystal structure with the Elongin B and Elongin C binding moiety (cyan) being replaced by a GSS linker to form ΔVif. The N terminal region of CBFβ that binds Cul5 (cyan) was also truncated to aid solubility. The N and C termini for Vif (yellow) CBFβ (grey) are labeled as N and C respectively. b) The araBad-pETDuet-1 vector map with inserted ΔVif (yellow) and ΔCBFβ (grey), c) Outline of the expression strategy. BL21(BE3) E. coli were transformed with the araBad-pETDuet-1 plasmid and grown in unlabeled medium. Induction of ΔCBFβ overexpression was done by addition of L-arabinose. For NMR active ΔVif, D-glucose was added to stop ΔCBFβ expression, then cell pellets were resuspended in either ^{15}N or $^{15}N/^{13}C$ enriched media, and ΔVif overexpression was induced by addition of IPTG.

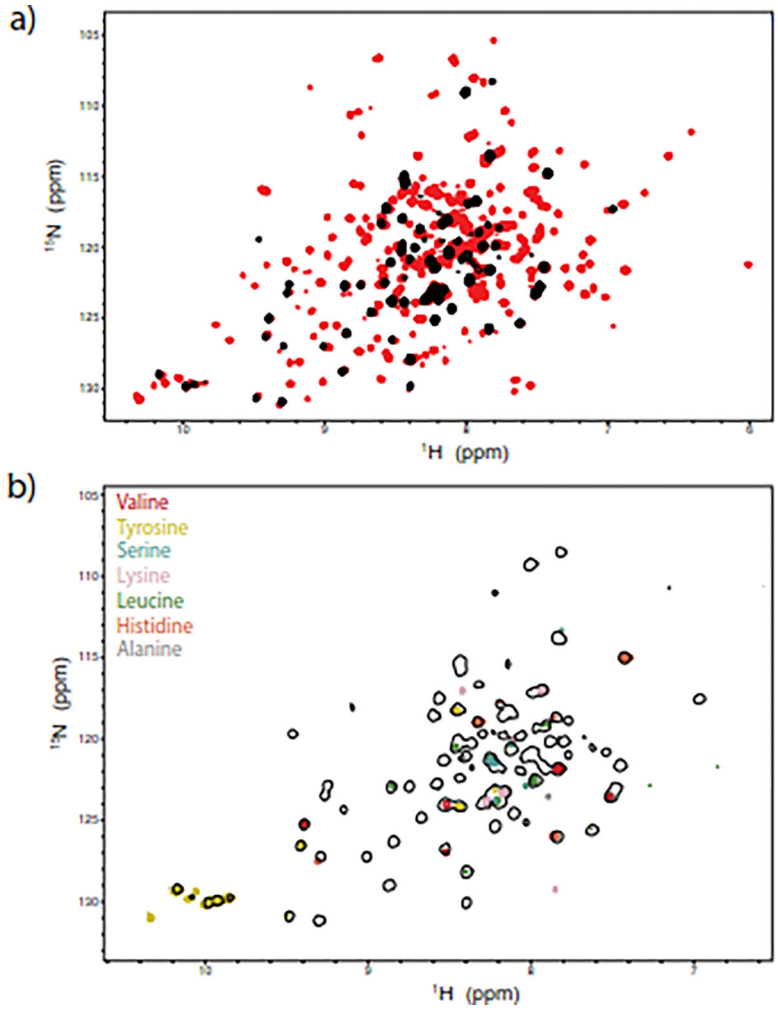

Figure 2.

a) Overlay of uniformly ^{15}N labeled ΔVif-ΔCBFβ complex (red) and ΔVif$^{\text{NMR active}}$-ΔCBFβ$^{\text{NMR inactive}}$ (black) ^{1}H-^{15}N TROSY-HSQC spectra. b) ΔVif signals with specific amino acid labeling are overlaid with a single contour spectrum of the ΔVif$^{\text{NMR active}}$-ΔCBFβ$^{\text{NMR inactive}}$. The spectra colors corresponding to amino acid type are indicated in the figure.

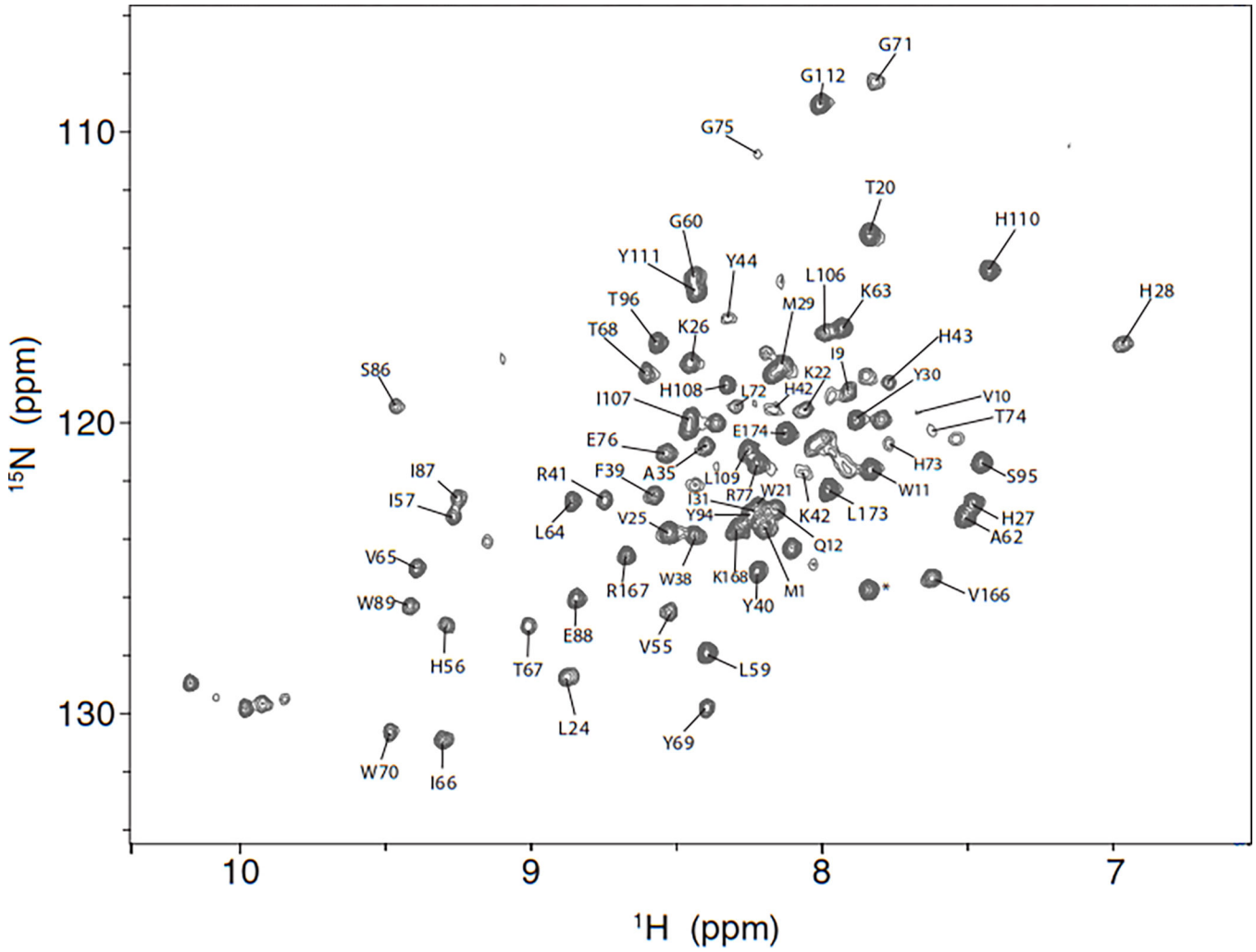

Figure 3.

^{1}H-^{15}N cross peak assignments of $\Delta Vif^{NMR\ active}$-$\Delta CBF\beta^{NMR\ inactive}$ on the ^{1}H-^{15}N TROSY-HSQC spectrum. * indicates a histidine in the 6xHis tag attached at the C-terminal of ΔVif.

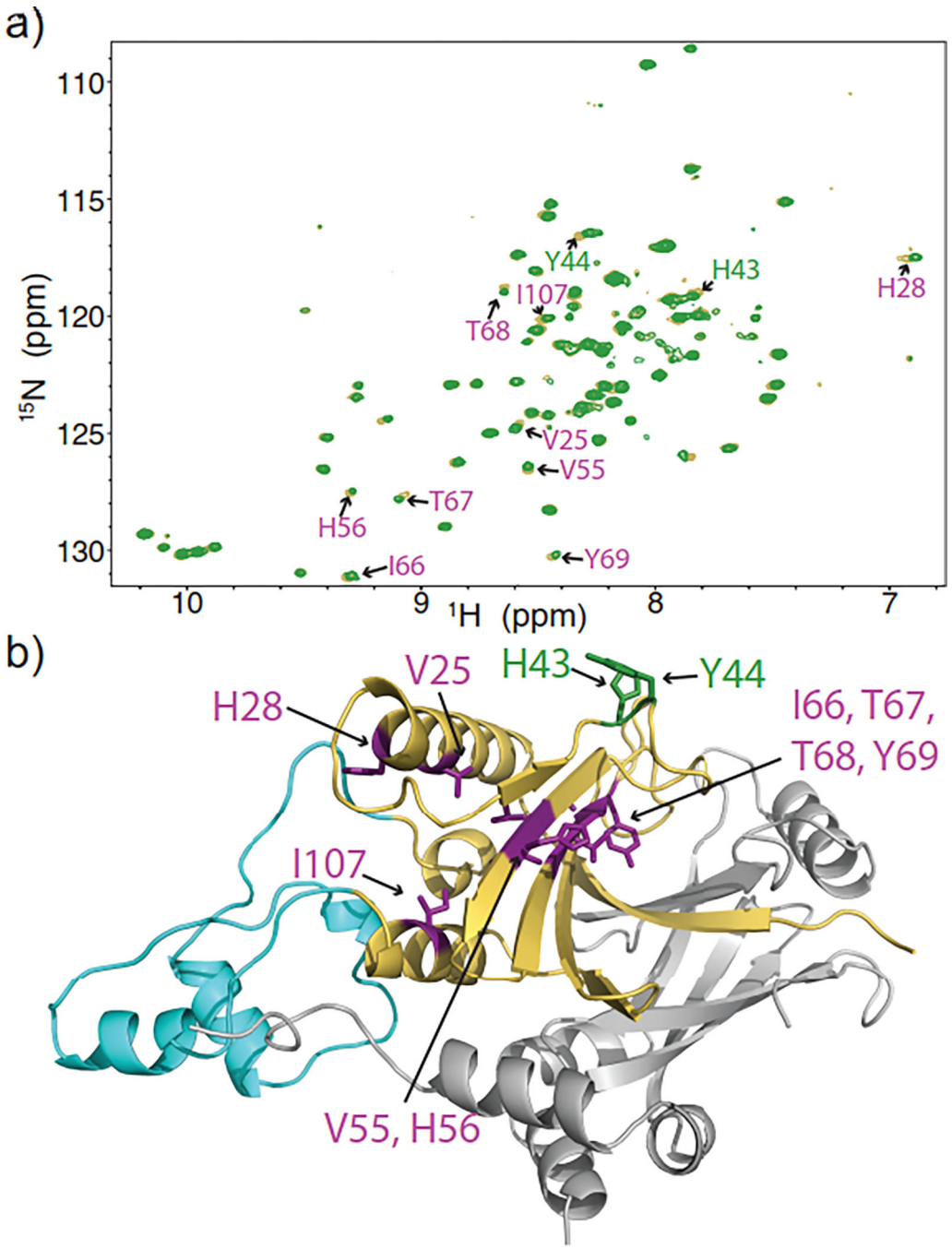

Figure 4.

a) ^{1}H-^{15}N TROSY-HSQC spectral overlay of ΔVif$^{\text{NMR active}}$-ΔCBFβ$^{\text{NMR inactive}}$ complex alone (yellow) and with A3G NTD-CTD2EA Y125A (Green). Green labels highlight H43 and Y44 surface exposed residues. Purple labels highlight interior residues. b) Amino acid residues on the interior (purple) and exterior (green) of ΔVif that show chemical shift perturbation on interacting with A3G NTD-CTD2EA Y125A are indicated as sticks on the cartoon drawing of the ΔVif (yellow) and ΔCBFβ (grey) complex.